Selective growth of Si/SiGe resonant tunneling diodes by atmospheric pressure chemical vapor deposition

A. Zaslavsky, D. A. Grützmacher, Y. H. Lee, W. Ziegler, and T. O. Sedgwick
IBM Research Division, T. J. Watson Research Center, Yorktown Heights, New York 10598

(Received 26 June 1992; accepted for publication 2 October 1992)

Atmospheric pressure chemical vapor deposition is used to grow *p*-type $Si/Si_{1-x}Ge_x$ double-barrier resonant tunneling structures on unstrained substrates, with a $Si_{0.75}Ge_{0.25}$ well clad by Si barriers. The current-voltage $I(V)$ characteristics at $T=77$ and 4.2 K exhibit current peaks and negative differential resistance regions corresponding to resonant tunneling through well-resolved heavy- and light-hole subbands in the well. Device quality is comparable to Si/SiGe resonant tunneling structures grown by molecular beam epitaxy. The *in situ* substrate cleaning and selective growth capabilities of atmospheric pressure chemical vapor deposition are used for the first successful selective growth of resonant tunneling structures through an oxide mask. The resulting diodes exhibit good resonant tunneling characteristics. The selective growth process is promising for the fabrication of small vertical heterostructure devices.

Rapid progress in the epitaxial growth of $Si/Si_{1-x}Ge_x$ heterostructures in recent years has stimulated considerable interest in the band-gap engineering possibilities in silicon. Many of the scientifically and technologically interesting heterostructures originally fabricated in III-V materials have already been replicated in $Si/Si_{1-x}Ge_x$, including double-barrier resonant tunneling diodes (RTD),[1-4] superlattices,[5] and modulation-doped two-dimensional (2D) electron and hole gases.[6-8] Compared to the most frequently studied $GaAs/Al_xGaAs_{1-x}$ III-V heterostructures, the band offsets available $Si/Si_{1-x}Ge_x$ are smaller, the greater lattice mismatch limits the critical thickness of strained layers, and larger effective masses reduce the attainable mobilities. On the other hand, in addition to the promise of band-gap-engineered silicon structures compatible with very large scale integrated (VLSI) technology, available silicon epitaxial growth and processing know-how combined with the existence of high-quality native oxide can lead to novel structures that are difficult to realize in III-V materials. In this letter we report on the first fabrication of *p*-type $Si/Si_{1-x}Ge_x$ RTD by atmospheric pressure chemical vapor deposition (APCVD).[9] The initial growth employed standard planar Si substrates and the current-voltage $I(V)$ characteristics of the resulting devices are comparable to *p*-type structures grown by molecular beam epitaxy (MBE),[1-3] indicating that APCVD can provide the layer thickness and uniformity control essential for high-quality heterostructures. Further, since APCVD allows for *in situ* substrate cleaning and selective growth normally not available in current alternative growth technologies, we have succeeded for the first time in selectively growing RTD structures in oxide windows. The resulting devices exhibit very good tunneling characteristics, indicating that selective growth by APCVD is a promising technique for the fabrication of Si-based heterostructure devices.

All of the devices were grown on heavily *p*-type doped Si substrates in the ASM Epsilon-1 APCVD system from dichlorosilane, germane, and diborane (for doping). For unpatterned substrates the growth sequence was as follows: after precleaning and loading into the chamber, the wafer was baked at 950 °C for oxide removal. The undoped RTD structures layers (with growth temperature T) were: 200 Å Si buffer (650 °C); 150 Å $Si_{1-x}Ge_x$ graded region with Ge content x ramped from 0 to 0.25 over the first 100 Å and maintained at $x=0.25$ over the last 50 Å (T ramped from 650 to 550 °C; 50 Å first barrier (650 °C); 60 Å $Si_{0.75}Ge_{0.25}$ well (550 °C); 50 Å Si second barrier (650 °C); 150 Å $Si_{1-x}Ge_x$ graded region with x ramped from 0.25 to 0 (T ramped from 550 to 650 °C). In the middle of this last graded layer diborane was gradually introduced, reaching a doping level of $\sim 5\times 10^{18}$ cm^{-3}, and a ~1000-Å-thick doped Si cap layer was grown (the doping was increased to $\sim 10^{20}$ cm^{-3} over the last 200 Å to facilitate contacts). The composition and growth rates of $Si_{1-x}Ge_x$ layers were calibrated by x-ray diffraction measurements on $Si/Si_{1-x}Ge_x$ superlattices.[10] The total thickness of the strained active region was below the critical thickness for $x=0.25$ (Ref. 11) and no dislocations were seen in transmission electron microscopy (TEM) cross-sectional micrographs. The 200 Å undoped Si buffer layer was grown to accommodate dopant diffusion from the substrate, which was otherwise found to destroy the resonant tunneling characteristics by shorting out the first barrier.

Figure 1 (a) shows a cross-sectional TEM photograph of the planar-grown, nonselective RTD structure. The uniformity and thickness control of the RTD structure layers grown by APCVD are very good. Ohmic contacts for $I(V)$ measurements were formed by Ti/Al metallization, with square top contacts ranging from $d=5$ to 300 μm on the side. These contacts served as a mask for reactive ion etching (RIE) used to isolate devices. Alternatively, passivated devices were fabricated by RIE mesa etching using photoresist as a mask, followed by low-temperature oxide deposition, and Ti/Al contact metal evaporation into lithographically defined windows on top of the device mesas. We found that oxide passivation has no appreciable effect on the RTD $I(V)$ characteristics.

The $Si/Si_{1-x}Ge_x$ RTD $I(V)$ characteristics were measured at $T=77$ and 4.2 K. The $I(V)$ curve at $T=4.2$ K of

 0003-6951/92/492872-03$03.00 © 1992 American Institute of Physics

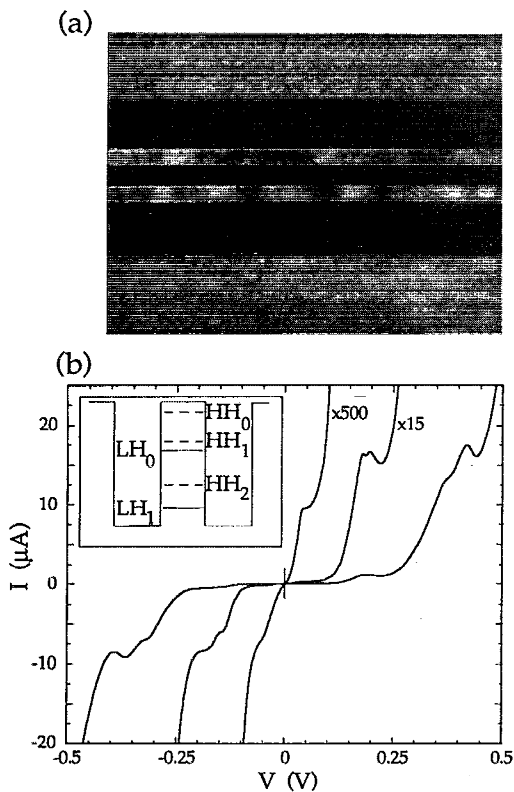

FIG. 1. (a) Cross-sectional TEM photograph of a planar-grown double-barrier RTD. The darker areas correspond to the strained $Si_{1-x}Ge_x$ layers. (b) Current-voltage characteristics of the $Si/Si_{0.75}Ge_{0.25}$ double-barrier RTD at T=4.2 K. Inset shows a schematic valence band diagram of the device, with the 2D heavy- and light-hole subbands in the well.

RTD device from the planar-grown wafer of Fig. 1(a) is shown in Fig. 1(b) (the T=77 K data are nearly identical, with slightly greater background leakage). In forward bias, with the top contact biased positive with respect to the substrate, we observe five resonant current peaks—or steps in the case of weaker peaks dominated by rising background current—at $V_{1,...,5}$=40, 180, 195, 370, and 420 mV; in reverse bias, the corresponding peaks are found at $V_{1,...5,}$ $=-50$, -145, -180, -315, and -365 mV. The large number of the resonant features arises from the relatively wide 60 Å $Si_{0.75}Ge_{0.25}$ well, which can accommodate two light-hole subbands LH_0 and LH_1, and three heavy-hole subbands $HH_{1,2,3}$, where the light and heavy designations label the effective mass in the tunneling direction. The current peaks occur as the 2D subbands in the well align with the occupied hole states in the $Si_{1-x}Ge_x$ emitter, enabling energy and transverse momentum-conserving tunneling. Although the strain in the $Si_{0.75}Ge_{0.25}$ causes a ~40 meV splitting between light- and heavy-hole valence band edges[2,12] and only the heavy-hole states are occupied at low temperatures in the emitter, we clearly observe tunneling through both heavy- and light-hole 2D subbands in the well. This indicates significant band mixing; the same effect was observed in MBE-grown devices by other groups.[1–3] Reliable assignment of resonant features to particular 2D light- and heavy-hole subbands is hindered by the complexity of the valence band dispersion in strained materials and

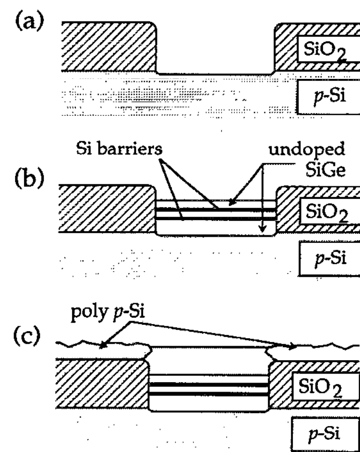

FIG. 2. Growth sequence for the selectively $Si/Si_{1-x}Ge_x$ RTD: (a) patterned oxide substrate; (b) selective growth of the undoped RTD structure in the oxide window, with no growth on the oxide; (c) growth of the p-dioped Si top contact layer. The p-doped Si material grown on the oxide mask is polycrystalline.

the nontrivial self-consistent potential distribution over the RTD.[13] The inset of Fig. 1(b) shows a schematic diagram of the 2D hole subband energies in the well with respect to the heavy-hole band edge, incorporating the ~40 meV heavy- and light-hole band edge splitting in $Si_{0.75}Ge_{0.25}$ and using a linear interpolation between Si and Ge values for the hole effective mass. In this oversimplified approximation, the resonant features at V_{1-5} can be assigned to HH_0, HH_1, LL_0, HH_2, and HH_1, respectively. The agreement between the observed and theoretically estimated bias positions of the resonant features is reasonable once we take into account the potential drop in the depletion region of the collector electrode of the RTD under bias.[13] The asymmetry between the peak positions in forward and reverse bias, which is smaller than is typically observed in nominally symmetric structures,[2,3] is due to the differences in the substrate and top electrode doping and in the doping profiles of the $Si_{1-x}Ge_x$ spacer layers outside the barriers.

The peak-to-valley ratios of the resonant features in Fig. 1 are comparable to the values observed in MBE-grown $Si/Si_{1-x}Ge_x$ RTDs,[1–3] confirming that APCVD can produce $Si_{1-x}Ge_x$ layers with sharp interfaces and good uniformity. An advantage of APCVD over the high-vacuum MBE and CVD techniques[1–4] lies in the *in situ* cleaning and selective growth capabilities, which we exploited to fabricate the first selectively grown RTDs using a patterned oxide mask. When the Si substrate is partially covered with oxide, undoped Si and $Si_{1-x}Ge_x$ material is only deposited on exposed Si.[14] Only when diborane is introduced into the chamber for p-type doping, does deposition on the oxide begin, as boron atoms stick to the oxide surface and provide nucleation centers for growth. Since our RTD design incorporates no doped buffer layers before the double-barrier structure, we can grow the devices selectively in oxide windows.

The device fabrication and selective RTD growth sequence is schematically shown in Fig. 2. Thermal ~1000-Å-thick oxide is grown on the substrate wafer. The oxide is

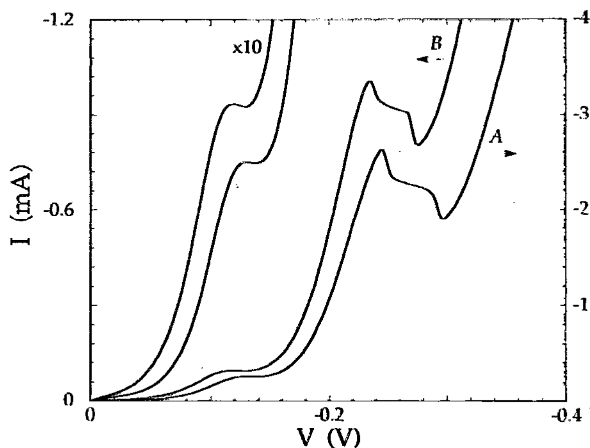

FIG. 3. The reverse bias $I(V)$ curves at $T=77$ K of RTDs selectively grown in $d=70$ μm (A) and 50 μm (B) oxide windows, together with their $\times 10$ expanded views.

lithographically patterned to open square windows of various sizes ($d=5$ to 300 μm) and RIE etched down to the substrate, whereupon the patterned wafer is loaded into the chamber [Fig. 2(a)]. After a high-temperature hydrogen clean, the undoped double-barrier structure is grown in the oxide windows, with no deposition on the oxide mask [Fig. 2(b)]. Only when p doping is introduced part-way though the top $Si_{1-x}Ge_x$ graded layer, does growth on the oxide mask commence. In the grown wafer the cap is polycrystalline on top of the oxide and single-crystal in the windows, as shown schematically in Fig. 2(c).

In calibration selective growth runs devices grown in oxide windows exhibited more misfit dislocations as the windows area became smaller. This is apparently due to a Ge "loading effect," i.e., an increase in the growth rate and Ge content x of Ge-containing layers grown in smaller oxide windows, which brings the total strained layer thickness closer to the critical thickness. A detailed study of this effect will be reported separately. In order to avoid dislocations in smaller selectively grown RTDs, the Ge content of $Si_{1-x}Ge_x$ layers was reduced by setting the growth parameters to the values that yield $x=0.18$ in planar-grown layers. As the growth rate of $Si_{1-x}Ge_x$ decreases with Ge content,[10] this reduced the well width to $\sim$30–40 Å in devices grown in $d\sim 100$ μm oxide windows. The reverse bias characteristics of two selectively grown devices ($d=70$ and 50 μm) are shown in Fig. 3, with strong resonant tunneling through HH_0 and LL_0 subbands. The narrower well in these devices spaces the resonant subbands further apart, enhancing the peak-to-valley ratios. The shift of the current peaks towards lower bias in the smaller device reflects the enhanced $Si_{1-x}Ge_x$ grown rate: the well is wider, which lowers the energy of quantized 2D subbands.

In the selectively grown wafer yielding the devices of Fig. 3, the defect density increased as the device size got smaller. In the smallest ($d=5$ μm) devices the entire area was heavily defective, leading to washed out $I(V)$ characteristics. However, as defect-free single-crystal Si was previously grown in $d\sim 1.5$ μm oxide windows in our system,[14] we believe the problem arises from insufficient cleaning of the Si surface in smaller oxide windows. An improved cleaning process should result in defect-free growth of RTDs and other $Si/Si_{1-x}Ge_x$ band-gap-engineered structures in small windows, down to the $d\sim 0.1$ μm scale.

In conclusion, we have employed APCVD to grow p-type $Si/Si_{1-x}Ge_x$ double-barrier resonant tunneling structures on unstrained Si substrates. Structures with a 60 Å $S_{0.75}Ge_{0.25}$ well clad by 50 Å Si barriers exhibit a number of resonant current peaks and negative differential resistance regions corresponding to hole tunneling through quantized heavy- and light-hole subbands in the well. The positions of the current peaks agree with simple tunneling theory and the $I(V)$ characteristics that APCVD-grown devices are of comparable quality to the MBE-grown structures reported by other groups.[1–3] Further, by employing the *in situ* cleaning and selective growth capabilities of APCVD, we have produced the first selectively grown RTDs in patterned oxide windows, which exhibited tunneling characteristics in no way inferior to planar-grown structures. With improvements in substrate cleaning and calibration of SiGe growth rates in small windows, the selective growth technique is expected to yield high-quality RTDs and other band-gap-engineered Si/SiGe structures in arbitrarily small oxide windows, potentially opening up new possibilities in the fabrication of laterally confined or gated vertical transport devices.

[1] H. C. Liu, D. Landheer, M. Buchanan, and D. C. Houghton, Appl. Phys. Lett. **52**, 1809 (1988); H. C. Liu, D. Landheer, M. Buchanan, D. C. Houghton, M. D'Iorio, and S. Kechang, Superlatt. Microstruct. **5**, 213 (1989).
[2] K. L. Wang, R. P. Karunasiri, J. Park, S. S. Rhee, and C. H. Chern, Superlatt. Microstruct. **5**, 201 (1989).
[3] U. Gennser, V. P. Kesan, S. S. Iyer, T. J. Bucelot, and E. S. Yang, J. Vac. Sci. Technol. B **8**, 210 (1990); **9**, 2059 (1991).
[4] K. Ismail, B. S. Meyerson, and P. J. Wang, Appl. Phys. Lett. **59**, 973 (1991).
[5] P. J. Wang, M. S. Goorsky, B. S. Meyerson, F. K. LeGoues, and M. J. Tejwani, Appl. Phys. Lett. **59**, 814 (1991).
[6] R. People, J. C. Bean, D. V. Lang, A. M. Sergeant, H. L. Stormer, K. W. West, R. T. Lynch, and K. Baldwin, Appl. Phys. Lett. **45**, 1231 (1984); P. J. Wang, B. S. Meyerson, F. F. Fang, J. Nocera, and B. Parker, *ibid.* **55**, 2333 (1989).
[7] G. Abstreiter, H. Brugger, T. Wolf, H. Jorke, and H.-J. Herzog, Phys. Rev. Lett. **54**, 2441 (1985).
[8] K. Ismail, B. S. Meyerson, and P. J. Wang, Appl. Phys. Lett. **58**, 2117 (1991); Y. J. Mii, Y. H. Xie, E. A. Fitzgerald, D. Monroe, F. A. Thiel, B. E. Weir, and L. C. Feldma, Appl. Phys. Lett. **59**, 1611 (1991); F. Schäffler, D. Többen, H.-J. Herzog, G. Abstreiter, and B. Holländer, Semicond. Sci. Technol. **7**, 260 (1992).
[9] T. O. Sedgwick, M. Berkenblit, and T. S. Kuan, Appl. Phys. Lett. **54**, 2689 (1989).
[10] D. A. Grützmacher and T. O. Sedgwick (unpublished).
[11] R. People and J. C. Bean, Appl. Phys. Lett. **48**, 538 (1986).
[12] R. People, Phys. Rev. B **32**, 1405 (1985); T. P. Pearsall, F. H. Pollak, J. C. Bean, and R. Hull, *ibid.* **33**, 6821 (1986).
[13] V. J. Goldman, D. C. Tsui, and J. E. Cunningham, Phys. Rev. B **35**, 9387 (1987); A. Zaslavsky, D. C. Tsui, M. Santos, and M. Shayegan, Phys. Rev. B **40**, 9829 (1989).
[14] T. O. Sedgwick, V. P. Kesan, P. D. Agnello, D. A. Grützmacher, D. Nguyen-Ngoc, and S. S. Iyer, IEDM Tech. Digest **1991**, 451.